Journal of Nano- and Electronic Physics
Vol. **18** No 3, 03006(6pp) (2026)

Журнал нано- та електронної фізики
Том **18** № 3, 03006(6cc) (2026)

REGULAR ARTICLE

Design and Optimization of a Compact 2D Photonic Crystal Filter with a Diamond-Shaped Cavity for Optical Sensing

F. Kebaili[1,*], A. Harhouz[1,†], H. Tayoub[1,2,‡], A. Hocini[1,§]

[1] *Laboratoire d'Analyse des Signaux et Systèmes, Faculty of Technology, Department of Electronics, University Pole, Bordj Bou Arreridj Road, 28000 Msila, Algeria*
[2] *Research Center in Industrial Technologie CRTI, P.O.BOX:64, Cheraga 16014 Algiers, Algeria*

(Received 25 January 2026; revised manuscript received 22 June 2026; published online 26 June 2026)

This paper presents the design, modeling, and simulation of an optical filter based on a two-dimensional photonic crystal (PhC), using RSoft software. The proposed structure consists of a periodic array of silicon rods incorporating a diamond-shaped central cavity. Numerical simulations were conducted to evaluate the influence of key parameters – such as rod radius, lattice periodicity, and substrate refractive index (RI) – on the spectral response of the filter. The study identified an optimal configuration (lattice period a = 0.45 μm, r_1 = 0.125 μm, r_2 = 0.08 μm), offering a good trade-off between compactness, selectivity, and quality factor. The results demonstrated the ability of the structure to produce sharp and well-defined resonance peaks, and highlighted the sensitivity of the resonant wavelength to the optical properties of the substrate material.

This work provides a relevant contribution to the design of efficient PhC filters and offers a solid technical foundation for further developments in integrated optics, particularly for applications in telecommunications and optical sensing.

Keywords: PhC filter, Cavity, FDTD, Optical filter, Optical sensing, Selectivity.

DOI: 10.21272/jnep.18(3).03006 PACS numbers: 07.05.Tp, 42.79.Ci

1. INTRODUCTION

In recent decades, photonic technologies have experienced tremendous growth, significantly impacting fields such as telecommunications, optical sensing, and information processing. Among the most promising emerging structures in this field, photonic crystals stand out for their remarkable ability to control and manipulate the propagation of light at the nanoscale, in a manner analogous to how semiconductors guide electron flow [1-5].

Thanks to their photonic bandgap, these structures enable the design of innovative, compact, and high-performance optical devices such as waveguides, microcavities, and especially optical filters. These filters play a crucial role in various applications, particularly in wavelength-division multiplexing (WDM) for optical communication systems and in the development of selective optical sensors, where precise wavelength selection is essential [6].

However, traditional optical filters face significant limitations, including poor integrability, sensitivity to the angle of incidence, and limited selectivity. These constraints have driven the search for alternative solutions, among which photonic crystal-based filters have emerged as a promising approach. Their periodic refractive index structure makes it possible to create photonic bandgaps where light propagation is prohibited. By introducing localized defects in this periodicity, it becomes possible to design highly selective and compact optical filters [7-15].

In this context, the present work focuses on the design, analysis, and simulation of a two-dimensional photonic crystal filter. To achieve this, we use RSoft, renowned for its capabilities in modeling integrated optical devices. With advanced simulation methods such as Finite Difference Time Domain (FDTD) and Beam Propagation Method (BPM), RSoft allows for precise analysis of the electromagnetic behavior of photonic structures and optimization of their optical and geometrical parameters.

2. FILTER DESIGN METHODOLOGY

2.1 Selection of Structural Parameters

The studied structure is a two-dimensional photonic crystal composed of a square lattice of air rods (refractive index n = 1) embedded in a silicon substrate with a refractive index of n = 3.45. The lattice periodicity, denoted a, is set to 0.45 μm, as shown in Fig. 1. The radius of the air rods is 0.1 μm, which corresponds to 22 % of the period. This configuration enables a well-defined photonic bandgap for transverse electric (TE) polarized waves (see Fig. 1).

* Correspondence e-mail: farida.kebaili@univ-msila.dz
† ahlam.harhouz@univ-msila.dz
‡ hadjira.tayoub@gmail.com
§ abdesselam.hocini@univ-msila.dz

Cite this article as: F. Kebaili et al., *J. Nano- Electron. Phys.* 18 No 3, 03006 (2026) https://doi.org/10.21272/jnep.18(3).03006

The structure consists of 31 rows and 30 columns, forming a 2D matrix of 930 rods in total. This configuration offers a good trade-off between simulation accuracy and computational time, while also allowing for the introduction of one or more localized defects within the matrix.

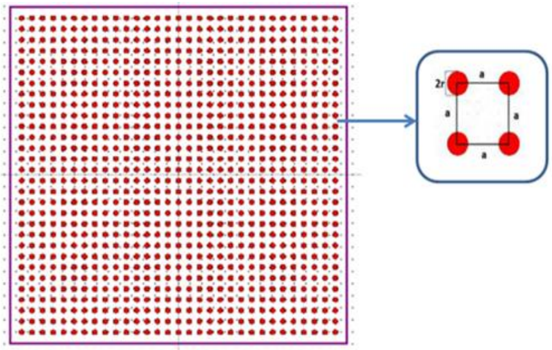

Fig. 1 – Schematic representation of the proposed two-dimensional photonic crystal structure

2.2 Analysis of the Influence of Lattice Periodicity on Photonic Band Gaps

To design a high-performance photonic crystal filter based on a square lattice of silicon rods in air (31 × 30 configuration), we investigated the effect of the lattice constant a on the photonic bandgaps, while keeping the rod radius constant at $r = 0.1$ µm. The simulation results reveal a significant evolution of the bandgaps depending on the value of a, as shown in Fig. 2.

For $a = 0.35$ µm, three photonic bandgaps are identified:

$TE_1 = [1.7241 – 1.1221]$ µm,
$TE_2 = [0.8280 – 0.6707]$ µm,
$TE_3 = [0.5265 – 0.5023]$ µm,

These results clearly show that the structure is capable of supporting multi-band operation.

When a is increased to 0.4 µm, only two photonic bandgaps are observed:

$TE_1 = [1.6200 – 1.1444]$ µm,
$TE_2 = [0.8543 – 0.7425]$ µm.

This reduction indicates that enlarging the lattice constant results in the disappearance of the higher-order bandgap.

With $a = 0.45$ µm, the bandgaps shift toward longer wavelengths:

$TE_1 = [1.7327 – 1.1597]$ µm,
$TE_2 = [0.8825 – 0.8302]$ µm.

This confirms that increasing the lattice constant results in a redshift of the bandgap positions.

Finally, for $a = 0.5$ µm, TE_1 continues to broaden ([1.8518 – 1.2195] µm), whereas TE_2 becomes very narrow ([0.7042 – 0.6849] µm), indicating a reduced efficiency in this range.

This analysis highlights a clear trend: increasing a causes a spectral shift (redshift) of the photonic bandgaps, with a notable broadening of TE_1. However, an excessively large value of a reduces the usefulness of TE_2. Therefore, a lattice constant of $a = 0.45$ µm represents the optimal trade-off, providing a wide TE_1 band well-positioned in the near-infrared range and a usable TE_2 band. This spectral positioning is particularly favorable for applications in optical telecommunications and biomedical sensing. Selecting this value ensures effective filtering, good spectral selectivity, and a compact structure.

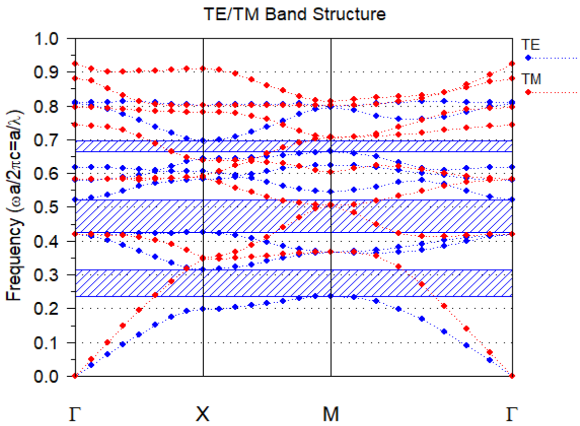

a

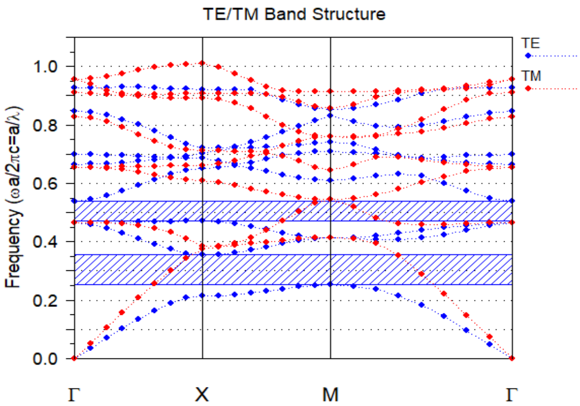

b

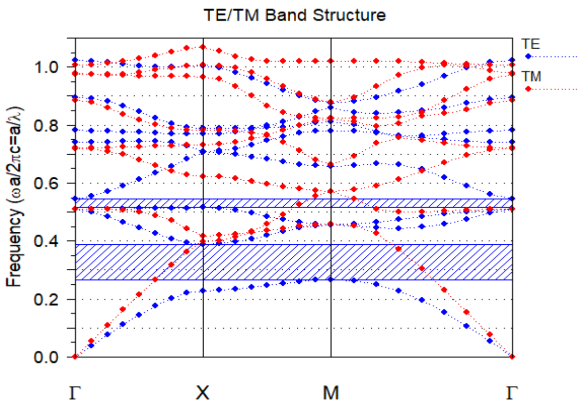

c

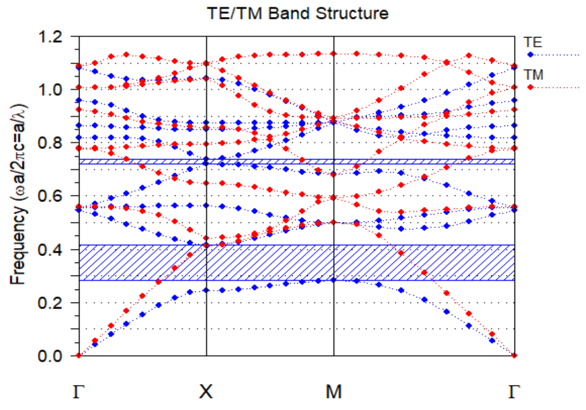

d

Fig. 2 – Band diagram schematic of the proposed two-dimensional photonic crystal structure for a = 0.35 (a), a = 0.4 (b), a = 0.45 (c), and a = 0.5 (d) respectively

2.3 Design of the Resonant Photonic Crystal Filter

The photonic crystal filter studied here was modeled using the RSoft software suite, based on a two-dimensional periodic structure composed of silicon rods in air, arranged in a 31 × 30 square lattice. This structure incorporates two lateral waveguides and a central diamond-shaped cavity, forming a resonant device specifically designed for the selective filtering of certain wavelengths (see Fig. 3).

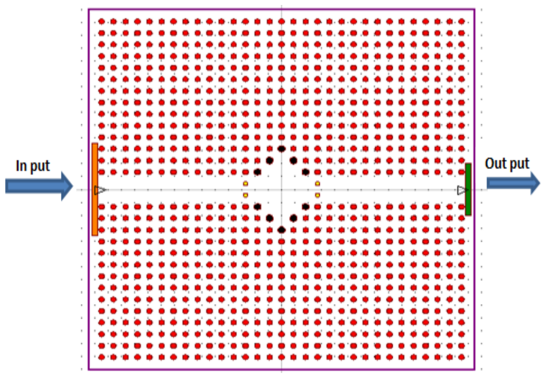

Fig. 3 – Schematic representation of the proposed filter

The input and output optical waveguides are created by removing twelve consecutive rods from each side of the structure: 12 rods at the input (left side) and 12 rods at the output (right side). These openings form two well-aligned optical channels that enable efficient light propagation, while the remaining rods in the photonic crystal ensure vertical confinement.

At the center of the structure, the resonant cavity is formed by removing 18 rods, resulting in a perfectly symmetrical diamond-shaped geometry. This configuration enhances electromagnetic field confinement and generates well-localized resonant modes within the cavity region. Surrounding the cavity, 14 rods were assigned specific radii to form the visible diamond pattern:

– 10 black rods with radius r_1, symmetrically placed along the diamond's edges. These play a key role in tuning the resonance and controlling field confinement.

– 4 yellow rods with radius r_2, located at the four corners of the diamond. They allow local modification of the effective refractive index, refining the filter's spectral selectivity.

This configuration results in a compact and well-defined cavity, clearly recognizable by its diamond shape, and efficiently coupled to the two waveguides through optimized geometric and optical continuity.

3. RESULTS OF THE SIMULATION

3.1 Study of the Effect of Radius R1 on the Spectral Response

In a photonic crystal without defects, waves with frequencies located within the photonic bandgap are completely reflected. However, when a defect is introduced, certain specific wavelengths are transmitted through the structure via guided modes.

The transmission coefficient is strongly influenced by the length of the defect, the excitation light profile, and the crystal termination type (boundary conditions). Simulating this behavior in RSoft allows visualization of the confined electromagnetic field in the channel and the transmission spectrum, which shows a peak within the bandgap.

Analysis of the transmission spectra obtained through simulation reveals the presence of two distinct peaks for each value of radius r_1, indicating the existence of two resonant modes in the cavity. This dual resonance is mainly due to the diamond-shaped geometry of the cavity and the symmetric distribution of the modified rods, which allow multiple possible configurations of the electromagnetic field.

According to Fig. 4, as the radius r_1 increases, both peaks gradually shift toward longer wavelengths, indicating a redshift effect caused by the increase in the local effective refractive index. This phenomenon enables spectral tuning of the filter by simply adjusting the size of the rods around the cavity. The study shows that r_1 is a key parameter in optimizing the filter, allowing control over the position, spacing, and quality of the resonance peaks.

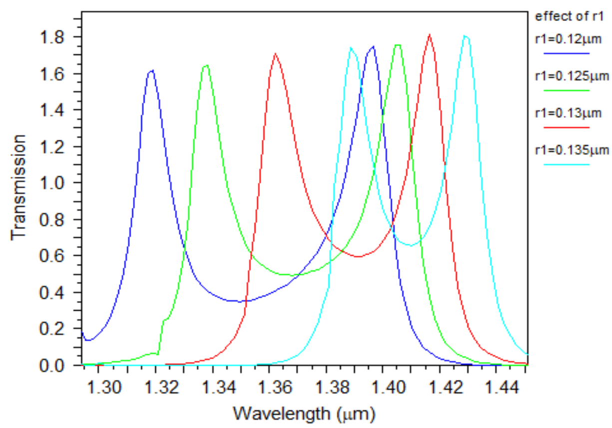

Fig. 4 – Output spectra of the filter for different values of radius r_1 with r_2 = 0.08 μm

This result confirms the effectiveness of the device in selecting a specific wavelength within the targeted operating range.

To evaluate the impact of radius r_1 on the response of the photonic crystal filter, several simulations were carried out by varying r_1 between 0.12 μm and 0.135 μm. The results show that changes in r_1 strongly affect the quality factor Q, and therefore the filter's selectivity.

For r_1 = 0.12 μm, r_1 = 0.13 μm, the Q values remain relatively low, around 3100, indicating weak confinement performance. In contrast, for r_1 = 0.125 μm, a clear improvement is observed with Q values exceeding 6700 for both peaks, reflecting good stability and enhanced filter selectivity.

Finally, for r_1 = 0.135 μm, the simulation shows a very high-quality peak with Q = 25543, but also a much weaker second peak with Q = 791.21, indicating strong asymmetry and spectral instability.

Thus, although the value r_1 = 0.135 μm allows achieving a very high-quality factor at a specific wavelength, the configuration offering the best compromise between performance and stability remains that with r_1 = 0.125 μm (see Table 1).

Table 1 – Variation of the resonant wavelength and quality factor as a function of radius r_1, with r_2 = 0.08 μm

r_1 [μm]	0.12	0.125	0.13	0.135
λ [μm]	1.3188/1.3963	1.338/1.4061	1.3621/1.4165	1.3891/1.4292
Q	3119/3114.3	6749.1/6544.5	3127.5/3127.5	25543/791.21

3.2 Study of the Effect of Radius r_2 on the Spectral Response

Table 2 and Fig. 5 show the impact of the secondary radius r_2 on the spectral response of the photonic crystal filter. As r_2 increases from 0.07 μm to 0.10 μm, the resonant wavelengths gradually shift to longer values. This redshift is not caused by a change in the refractive index of the materials themselves, but rather by the increase in the volume fraction of the high-index material (silicon) within the unit cell. This leads to an increase in the effective refractive index of the periodic structure, which alters the photonic bandgap and shifts the resonance conditions.

Regarding performance, the quality factor Q – which indicates the sharpness and efficiency of the resonance – varies significantly with r_2. For r_2 = 0.07 μm, the filter exhibits a very high Q-factor (5793.5) at the first resonance, but a very low value (67.08) at the second, indicating possible mode leakage or poor confinement.

The optimal performance is achieved at r_2 = 0.08 μm, where both resonance peaks exhibit very high and well-balanced quality factors (6749.1 and 6544.5). This demonstrates excellent mode confinement, high spectral selectivity, and minimal energy loss – making this radius the most suitable for efficient filter design.

Beyond this value, for r_2 = 0.09 μm and 0.10 μm, the quality factor drops significantly (around 116 and 128), suggesting degraded filtering performance, likely due to increased radiation losses or mode leakage.

Table 2 – Variation of the resonant wavelength and quality factor as a function of radius r_2, with r_1 = 0.125 μm

r_2 [μm]	0.07	0.08	0.09	0.1
λ [μm]	1.333/1.4	1.338/1.40681	1.342/1.4097	1.3464/1.4132
Q	5793.5/67.08	6749.1/6544.5	116.92/116.92	128.42/128.07

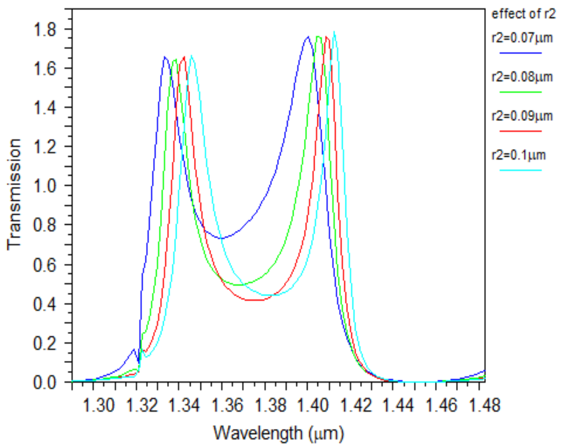

Fig. 5 – Output spectra of the filter for different values of radius r_2 with r_1 = 0.125 μm

3.3 Study of the Effect of the Refractive Index on the Spectral Response

The results presented in Table 3 and Figure 6 highlight the impact of the material's refractive index nn on the spectral behavior of the photonic crystal filter. As nn increases gradually from 3.39 to 3.48, the resonant wavelengths shift toward longer values, producing a redshift in the spectrum. This effect occurs because light travels more slowly in a medium with a higher refractive index, thus modifying the optical path and the resonance conditions within the photonic structure.

In parallel, the quality factor Q shows a non-monotonic evolution. At n = 3.39, the filter exhibits a very high Q-factor (4737.8) at the first resonance, but a much lower value (87.954) at the second one, revealing a possible asymmetry in mode confinement. For n = 3.42, both resonances yield extremely low Q-factors (≈ 91.4), indicating poor spectral selectivity and energy leakage.

Surprisingly, the best performance is achieved at n = 3.45, where both resonant modes show very high and symmetric quality factors (6749.1 and 6544.5), demonstrating excellent mode confinement, high finesse, and narrow resonance peaks. This value corresponds to the optimal refractive index for the given filter configuration.

However, further increasing the index to n = 3.48 results in a significant drop in the quality factor (87.73 / 98.682), indicating a degradation of resonance sharpness, possibly due to increased radiation losses or mismatched mode coupling.

These observations confirm that the choice of the refractive index is a crucial design parameter, as it directly influences both the position and sharpness of the resonant peaks, and thus, the overall efficiency of the photonic filter.

Table 3 – Variation of the resonance wavelength and quality factor as a function of the refractive index

n	3.39	3.42	3.45	3.48
λ [μm]	1.3283/1.3992	1.3336/1.4025	1.338/1.4061	1.3434/1.4089
Q	4737.8/87.954	91.400/91.399	6749.1/6544.5	87.73/98.682

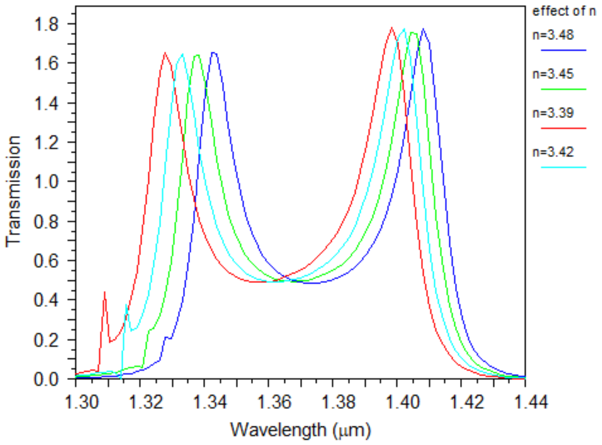

Fig. 6 – Output spectra of the filter for different refractive index values

Table 5 shows a comparison between the proposed filter and several published articles. Our results are highly satisfactory, considering quality factor.

Table 5 – Comparison of our results with published references

reference	Q
[6]	4638.78
[12]	1823
[10]	256
This work	6749.1

4. CONCLUSION

This work has highlighted the great potential of photonic crystals in the design of next-generation optical devices, focusing particularly on the development of a two-dimensional optical filter. Thanks to their ability to control light propagation through the photonic bandgap, these structures stand out as promising solutions in fields such as telecommunications, optical sensing, and integrated photonics.

Using the RSoft simulation platform, we designed and numerically analyzed a photonic crystal-based filter. We first investigated the effect of lattice periodicity on bandgap formation, revealing a redshift in the photonic bandgap with increasing lattice constant. An optimal compromise was found for a lattice constant of $a = 0.45$ μm, yielding a wide TE1 band in the near-infrared range, well-suited for optical communication applications.

We then examined the influence of various geometric and optical parameters on the filter's performance. The radius $r_1 = 0.125$ μmr around the cavity was found to provide excellent stability and high performance, with a quality factor exceeding 6700. Additionally, tuning the radius r_2 confirmed its role in fine-tuning the resonance, with the best selectivity obtained at $r_2 = 0.08$ μm. Finally, the analysis of the refractive index effect revealed a progressive redshift of the resonance wavelength and a decrease in the quality factor as the refractive index increased, as summarized in Table 4 and illustrated in Figure 6. These results confirm that careful selection of physical parameters allows for effective optimization of the filter's spectral response.

In summary, this study has demonstrated the effectiveness of photonic crystals in the development of compact and high-performance optical filters, while also showcasing the power of numerical simulation tools such as RSoft in the design process.

Moreover, this work opens the door to several future perspectives. Further investigations could focus on three-dimensional or quasi-periodic structures, the intentional introduction of defects to tailor resonant properties, or the integration of such filters into complete photonic circuits. Exploring active or nonlinear materials may also enhance filter performance and broaden their application range.

REFERENCES

1. A. Harhouz, A. Hocini, *J. Electromagn. Waves Appl.* **29** No 5, 659 (2015) https://doi.org/10.1080/09205071.2015.1012597.
2. A. Hocini, A. Harhouz, *J. Nanophoton.* **10** No 1, 016007 (2016) https://doi.org/10.1117/1.JNP.10.016007.
3. H. Tayoub, A. Hocini, A. Harhouz, *J. Nano- Electron. Phys.* **13** No 6, 06005 (2021) https://doi.org/10.21272/jnep.13(6).06005.
4. F. Kebaili, A. Harhouz, A. Hocini, *Progr. Electromagn. Res. C* **140**, 85 (2024) http://doi.org/10.2528/PIERC23120502.
5. F. Kebaili, Abdesselam Hocini, Ahlam Harhouz, *Phys. Scripta* **100**, 065518 (2025) https://doi.org/10.1088/1402-4896/add4b1.
6. O. El Mansouri, A. Labbani, *J. Microwaves, Optoelectron. Electromagn. Appl.* **23** No 1, e2024280819 (2024) https://doi.org/10.1590/217910742024v23i1280819.
7. S. Muhammad, D. Chen, C. Xian, J. Zhou, Z. Lei, P. Kuang, Z. Li, G. Wen, Y. Huang, *Photonics* **11**, 753 (2024) https://doi.org/10.3390/photonics11080753.
8. S. Robinson, R. Nakkeeran, *Opt.- Int. J. Light Electron Opt.* **124** No 18, 3430 (2013) https://doi.org/10.1016/j.ijleo.2012.10.038.
9. A. Rostami, H. Alipour Banaei, F. Nazari, A. Bahrami, *Optik* **122** No 16, 1481 (2011) https://doi.org/10.1016/j.ijleo.2010.05.036.
10. K. Venkatachalam, D. Sriram Kumar, S. Robinson, *J. Biopolym. Theor. Stud.* **2**, 39 (2022).
11. M. Mohammadi, M. Seifouri, *Opt. Quant. Electron.* **51**, 350 (2019) https://doi.org/10.1007/s11082-019-2061-z.
12. K. Venkatachalam, S.K. Dhamodharan, S. Robinson, *J. Opt. Commun.* **43** No 4 (2018) https://doi.org/10.1515/joc-2018-0216.
13. A. Labbani, I. Moumeni, F. Bounaas, *WSEAS Trans. Electron.* **10**, 122 (2019).
14. F. Kebaili, A. Harhouz, A. Hocini, *J. Microwaves, Optoelectron. Electromagn. Appl.* **24** No 1, e2024289725 (2025) https://doi.org/10.1590/2179-10742025v24i1289725.
15. H. Tayoub, A. Harhouz, A. Hocini, *Phys. Scripta* **98**, 115510 (2023) https://doi.org/10.1088/1402-4896/acff29.

Проєктування та оптимізація компактного 2D фотонно-кристалічного фільтра з ромбоподібною порожниною для оптичного зондування

F. Kebaili[1], A. Harhouz[1], H. Tayoub[1,2], A. Hocini[1]

[1] *Laboratoire d'Analyse des Signaux et Systèmes, Faculty of Technology, Department of Electronics, University Pole, Bordj Bou Arreridj Road, 28000 Msila, Algeria*

[2] *Research Center in Industrial Technologie CRTI, P.O.BOX:64, Cheraga 16014 Algiers, Algeria*

У роботі представлено проєктування, моделювання та симуляцію оптичного фільтра на основі двовимірного фотонного кристала (ФК) за допомогою програмного забезпечення RSoft. Запропонована структура складається з періодичного масиву кремнієвих стрижнів, що містять ромбоподібний центральний резонатор. Чисельне моделювання було проведено для оцінки впливу ключових параметрів, таких як радіус стрижня, періодичність решітки та показник заломлення підкладки (ПЗ) на спектральну характеристику фільтра. Дослідження визначило оптимальну конфігурацію (період решітки a = 0.45 мкм, r_1 = 0.125 мкм, r_2 = 0.08 мкм), що пропонує хороший компроміс між компактністю, селективністю і коефіцієнтом якості. Результати продемонстрували здатність структури створювати різкі та чітко визначені резонансні піки, а також підкреслили чутливість резонансної довжини хвилі до оптичних властивостей матеріалу підкладки. Ця робота є важливим внеском у проєктування ефективних ФК-фільтрів та пропонує міцну технічну основу для подальшого розвитку інтегральної оптики, зокрема для застосувань у телекомунікаціях та оптичному зондуванні.

Ключові слова: PhC-фільтр, Резонатор, FDTD, Оптичний фільтр, Оптичне зондування, Селективність.